Structure, Vibrations and Raman Modes in Electron Doped Metal Phthalocyanines[†]

Jaroslav Tóbik*[,‡] and Erio Tosatti[‡,§]

International School for Advanced Studies (SISSA), and INFM Democritos National Simulation Center, Via Beirut 2-4, I-34014 Trieste, Italy, and The Abdus Salam International Centre for Theoretical Physics (ICTP), P.O. Box 586, I-34014 Trieste, Italy

Received: July 27, 2007; In Final Form: October 11, 2007

Identifying and understanding the vibrational frequency shifts caused by electron addition to metal phthalocyanine (MPc) molecules is the main goal of the present work. Among other things, it should be useful in establishing the amount of charge-transfer level recently reported in potassium doped solid MPc films. Choosing MgPc as our working case, we calculated by density functional methods the full vibration spectrum of the neutral and of the negatively charged molecule, with and without Jahn−Teller distortion. In the negative ion MgPc$^-$ we found that although individual modes behave differently, the generality of modes undergoes a negative frequency shift of about 10 cm^{-1} for a single extra electron added in the e_g affinity level. We calculated the Raman intensities and made qualitative connection with recent data on K-doped CuPc films. The detailed features and parameters of the static Jahn−Teller effect in a phthalocyanine molecular ion are obtained as a byproduct.

1. Introduction

The possibility of building novel metals by doping molecular crystals has generated excitement for decades already. Among others the cases of polyacetylene, fullerenes, TTF-TCNQ, (TMTSF)$_2$X, (TMTTF)$_2$X, and (BEDT-TTF)$_2$X salts, etc., have brought out so far several remarkable pieces of physics.[1]

Recent work suggested that films of transition metal phthalocyanines (MPcs) CuPc, NiPc, CoPc, FePc, MnPc, initially insulating, can be turned metallic through potassium doping. Schematic structure of MgPc is shown on Figure 1. An increasing level of *K* doping is believed to enact a charge transfer from zero to four electrons per MPc molecule,[2,3] largely to the 2-fold degenerate e_g lowest unoccupied molecular orbital (LUMO).[4,5] In simple but realistic model crystal structures, this orbital gives rise to narrow bands.[6] In the presence of doping the simplest rigid band model can explain, as proposed by refs 2 and 3, why the MPcs, initially insulating when pristine ($n = 0$)[7] may end up again as insulators at full doping ($n = 4$) but are metallic in between.

The main other example of *K*-doping induced metalization are the alkali metal fullerides, an important class of compounds that includes Mott insulators, metals, and superconductors, and which have generated a large amount of literature.[8] Although at this stage it is not yet clear whether stoichiometric compound phases exist for MPcs as they do in the fullerides, there appears to be, at least potentially, a close analogy. Even the conductance reported at KMPc optimal metallic doping is very close in magnitude and temperature (in)dependence to that of K$_3$C$_{60}$ films.[2]

An important element in the future search for well-defined compounds will be the possibility to establish, to the best

possible degree of approximation, the doping level—that is, the amount of electronic charge acquired by the e_g level of each molecule. Vibrational shifts observed by infrared and Raman spectroscopy have been successfully used in determination charge-transfer state, for example, in TTF molecules.[9] In the case of fullerene, there is a well documented approximately linear connection between the doping level and the vibrational frequency shifts,[10,11] a scale that is widely used for example for adsorbed molecules on surfaces. A similar scale would be very useful for Mpcs as well. Recent Raman data were published for K$_x$CuPc, although the exact doping concentration x is not precisely specified.[2]

The scope of the present calculation is manifold. First, we will apply standard density functional theory (DFT) methods to calculate the electronic states, the optimal geometry, the full vibrational spectrum, and the relative Raman and infrared intensities of a neutral MgPc molecule. Second, we shall attempt to predict the changes of all these properties caused by the addition of one electron to the molecular e_g level, mimicking the minimal effect of electron doping. In the process, we will describe quantitatively the static Jahn−Teller (JT) effect in the MgPc$^-$ ion.

To avoid difficulties with transition metals MPcs that generally display open shells of d orbital character in the HOMO−LUMO gap (see Figure 2 in ref 4), we choose to work with the nonmagnetic metal phthalocyanine molecule MgPc, which makes for a particularly simple reference case. The lack of open d shells (as in CuPc), or of semicore filled d shells (such as in ZnPc) allows us to use simple LDA and a relatively modest plane wave basis rather than computationally heavier approaches.

We are of course not the first to consider the JT effect in MgPc$^-$ anion. Besides ref 4, the electronic structure of the MgPc anion was discussed by Cory et al.[12] That paper, however, appears to assume an unrealistic symmetry for the JT active modes. We will return to this point in the discussion.

Electron Doped Metal Phthalocyanines

J. Phys. Chem. A, Vol. 111, No. 49, 2007 **12571**
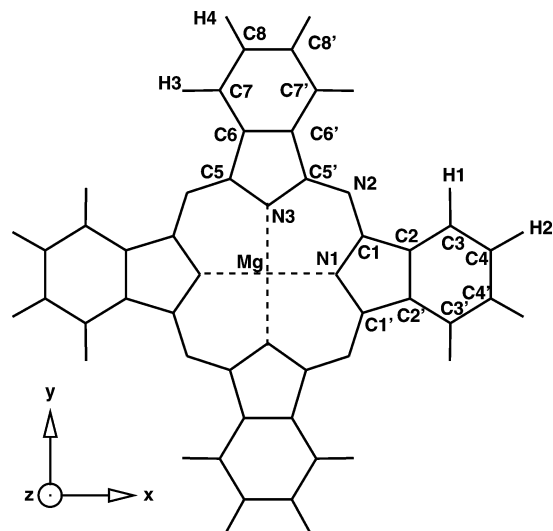
Figure 1. Schematic of the MgPc and MgPc$^-$ molecule.
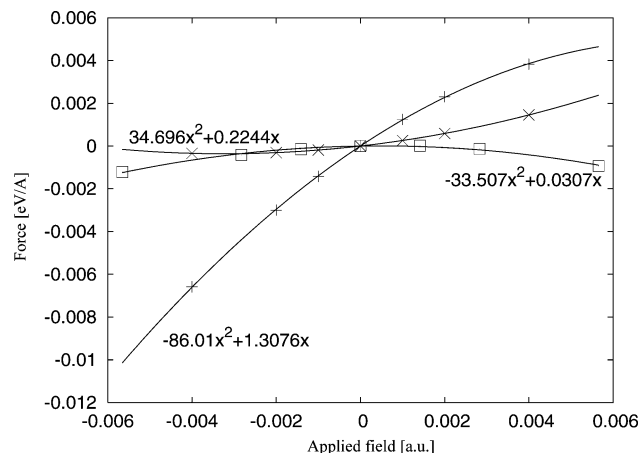
Figure 2. x component of the force acting on atom C_2 (for notation see Figure 1) upon applied external field in the x direction (pluses), y direction (times), and xy direction (squares). A reasonable fit by quadratic dependence is demonstrated.

Our choice of MgPc instead of, e.g., ZnPc is also motivated by some uncertainty about the ZnPc structure. ZnPc was at some stage believed to be nonplanar even in the gas phase.[13] A later reinvestigation in the gas phase established a planar structure, also confirmed by calculations (see ref 14 and references therein). Nonetheless, calculations by Tackley et al.[15] indicate a slightly nonplanar structure. For a symmetrized molecule with D_{4h} symmetry they obtained imaginary frequencies corresponding to negative curvature of the total energy along unstable normal coordinates. So this leaves some doubts about the planarity of ZnPc. MgPc, in its crystalline β structure, is known to dimerize with strong out-of-plane deformation.[17] This dimerization permits a higher coordination of the central metal atom to nitrogen of the nearest molecule in the molecular stack and is thus a strict consequence of the β crystal structure. It would thus be absent in the α structure where that coordination is absent. In that respect, we recall that the MPc films that were subsequently K-doped were reportedly undimerized α structures.[2] Our own DFT calculations, moreover, do yield a planar structure for the neutral molecule. A planar structure of neutral MgPc is experimentally reported in ref 14. For the charged molecule some soft or marginally imaginary modes were found corresponding to out-of-

plane vibrations.[18] Nonplanarity of the anion could in principle arise through a Renner–Teller effect.[19] That kind of effect is, however, second order and would therefore be even weaker with respect to an already weak first-order Jahn–Teller effect. We neglected these effects altogether by keeping the anion structure planar throughout.

The 2-fold e_g LUMO degeneracy, common in metal phthalocyanines and porphyrins, leads in the presence of an added electron to an open shell problem with orbital degeneracy and a JT effect. On account of that, the anion calculations will be realized in two different instances.

The first is the static JT instance, where the molecule is allowed to statically distort from D_{4h} to D_{2h} symmetry. The extra electron occupies one of the two formerly degenerate e_g sublevels, now split, spin polarized, and lowered in energy by the symmetry breaking distortion. The change of molecular symmetry is expected to affects heavily all vibrational modes, as is indeed found. However, this calculation is at best of heuristic value for two reasons. This is the first reason that, due to intrinsic limitations of DFT, this kind of calculation will tend to underestimate somewhat the actual JT energy gain, the symmetry breaking distortion magnitude, and even more the e_g level splitting. The JT splitting becomes here the fundamental gap of this system, and DFT is affected by a "gap problem". There exist more complex schemes (such as GW) that can remedy some of these problems; however, they are elaborate and we cannot consider them here.

A different and more fundamental reason is that even at absolute zero the quantum motion of the nuclei will cause the molecular ion coordinates to tunnel between equivalent but different distortion minima. That tunneling generally transforms the JT effect from static to dynamic, in the process fully restoring the D_{4h} static molecular symmetry, while gaining some extra amount of ionic zero point energy. Ion quantum mechanics is not considered in the present study, where ionic coordinates are treated classically. A full study of the dynamic JT effect in MgPc$^-$ goes well beyond the scopes of this work and must be left for future work, worth embarking in if there will be experimental interest.

The second instance we will consider as a counterpart to the first is the undistorted negative ion, artificially stabilized by means of fractional occupancies. In practice, half a nominal electron is added to each of the two degenerate e_g sublevels, so that the original molecular D_{4h} symmetry is preserved by construction. At the price of neglecting all JT and spin polarization effects, it then becomes very easy in this approximation to follow the shifts of frequency and intensity that all modes undergo on average upon doping.

Finally, the calculated frequency shifts can be compared with those recently observed for a few Raman modes in KCuPc relative to pristine CuPc, which will allow some tentative conclusions about a frequency-doping scale in MPcs.

2. Method

Electronic structure calculations for MgPc and MgPc$^-$ were carried out using the PWscf software package, a plane-wave density functional implementation[20] in the local density approximation (LDA). We used ultrasoft pseudopotentials of the RRKJ3 form[21] with a cutoff energy of 35 Ry for the basis set wave functions and 280 Ry for the electron density. A single magnesium phthalocyanine MgPc molecule was embedded in a periodically repeated artificial supercell of size $21 \times 21 \times$

12572 *J. Phys. Chem. A, Vol. 111, No. 49, 2007*

Tóbik and Tosatti
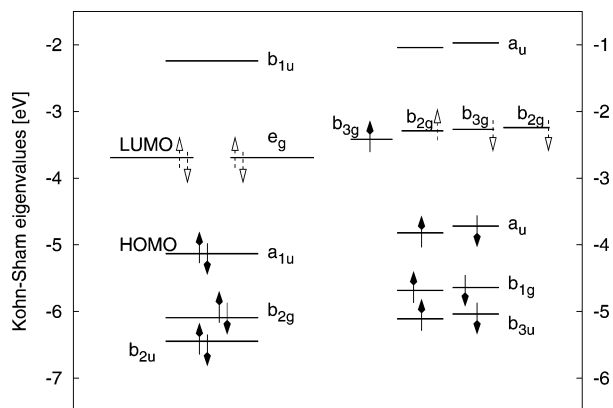
Figure 3. Relevant ground state electronic levels of neutral MgPc (left) and of the Jahn−Teller distorted, spin−polarized MgPc$^-$ molecular ion (right). Energies are referred to vacuum zero (obtained as the extrapolated Hartree potential at infinity). Note the shifted energy scale for the charged molecule. The Jahn−Teller orbital splittings are 126 meV ($b_{3g}\uparrow - b_{2g}\uparrow$). Occupation and spin polarization of the levels is indicated by arrows. Empty orbitals are indicated by a dashed arrow with an empty head; occupied, by a full line arrow and filled head.

10 Å, which can be considered large enough to represent the molecule in a vacuum.

MgPc$^-$ ion calculations were done similarly, by adding an extra electron to the neutral molecule, but now allowing for overall spin polarization caused by the unpaired spin, and treated within LSDA (spin unrestricted LDA). We avoided introducing potassium ions of uncertain location, and overall charge neutrality was instead enforced by assuming a uniform positive neutralizing background. Fractional occupancy of the symmetric negative ion was done using the density functional with fractional occupation numbers, by means of the nonzero "electronic" temperature technique as introduced in ref 22. Algorithmic implementation of minimization in this functional made use of the Marzari−Vanderbilt scheme.[23] Because the gap between LUMO e_g and HOMO b_{1u} is about 1.4 eV, we found that an electronic temperature of 0.3 eV was enough to occupy only the desired e_g states.

Following the electronic structure calculations, linear response theory was subsequently applied for the calculation of full molecular vibrational spectra.[24] The dynamical matrix was constructed making use of all symmetry restrictions, based on D_{4h} (MgPc and undistorted MgPc$^-$) or on D_{2h} (JT distorted MgPc$^-$) groups. Only independent matrix elements were calculated.

Once the dynamical matrix was diagonalized and all vibrational modes obtained, we calculated the Raman spectral intensity of the active modes. In the semiclassical approximation, we calculated for that purpose the change of (low frequency) molecular polarizability tensor $\alpha_{\mu\nu}$ caused by each vibrational normal mode (of coordinates q_i),[25] which dynamically modulates the dielectric response and causes the inelastic light scattering. In terms of these quantities the Raman tensor is simply defined as $T^i_{\mu\nu} = \partial\alpha_{\mu\nu}/\partial q_i$. The static polarizability α of the molecule is in turn the second derivative of its total energy U with respect to an applied electrostatic field F_μ. Thus the Raman tensor is made up of third derivatives of total energy. In our implementation we first calculated analytically the Hellmann−Feynman forces, that are first derivatives of total energy with respect to atomic displacements. We did that in the explicit presence of an external electrostatic field, and for variable field strength. Fitting the force dependence upon the field by a second-order polynomial, we obtained numerically the second derivatives of the forces with respect to the field. A typical force dependence on the electrostatic field is shown in Figure 2, showing as an

example how the force along x direction on atom C_2 depends upon the external field applied in directions x, y, and xy (the atom notation and coordinate orientation are shown in Figure 1). For each individual vibrational normal mode, we combined contributions to each Raman tensor component from the displacement of every atom in the molecule.

Details of the application of electrostatic fields within periodic boundary conditions are the same as given elsewhere.[26] We note that it would of course have been possible to obtain alternatively the desired energy derivatives by density functional perturbation theory (DFPT), as was done, e.g., by Deinzer et al.[27] or by Lazzeri et al.[28] Our numerical derivatives and DFPT are conceptually equivalent and do in every respect lead to the same result. We just found numerical derivatives simple and straightforward to implement in the present case.

Given the Raman tensor $T^i_{\mu\nu}$ the (non-resonant) Raman scattering cross section is given by[25,29]

$$\frac{d\sigma_i}{d\Omega} = \frac{(2\pi\nu_0)^4}{c^4} \frac{h(n_i + 1)}{8\pi\nu_i} \frac{45\alpha'^2_i + 7\gamma'^2_i}{45}$$

$$\alpha'_i = \frac{1}{3}(T^i_{xx} + T^i_{yy} + T^i_{zz})$$

$$\gamma'^2_i = \frac{1}{2}\{(T^i_{xx} - T^i_{yy})^2 + (T^i_{xx} - T^i_{zz})^2 + (T^i_{yy} - T^i_{zz})^2 + $$

$$6[(T^i_{xy})^2 + (T^i_{xz})^2 + (T^i_{yz})^2]\}$$

$$n_i = \left[\exp\left(\frac{h\nu_i}{kT}\right) - 1\right]^{-1} \qquad (1)$$

Here ν_0 is the frequency of incident light and n_i is the occupation number of vibrational state i at temperature T. The symbols α' and γ'^2 are the isotropic and anisotropic part of scattering process, which arise from a directional average assuming a uniformly distributed random orientation of the molecule. Numerical prefactors (45 and 7) depend on the experimental geometry. They were chosen for the most common experimental setup, when incident light, direction of observation, and vector of electric intensity of incident light are all perpendicular to each other.[25]

For completeness we also calculated infrared absorption amplitudes. These are related to vibration induced dipole momenta. In the framework of the total energy IR absorption intensity

$$p'_\mu = \frac{\partial^2 U}{\partial q_i \partial F_\mu} \qquad (2)$$

is related to amplitude of dipole moment vector induced by vibration i, where again U is total energy and F_μ is the vector component of the applied external electrostatic field. Derivatives were obtained by fitting linear coefficients of force dependence upon the applied electrostatic field. These coefficients were combined with proper weights to get derivatives with respect to each vibrational normal coordinate q. The infrared absorption intensity is then proportional to the square of the amplitude of the induced dipole moment $I^{IR} \propto |\vec{q}'|^2$.[29,30]

$$I^{IR} = \frac{N\phi}{3c} |\vec{p}'|^2 \qquad (3)$$

where N is the number of particles and c is the speed of light.

Electron Doped Metal Phthalocyanines

J. Phys. Chem. A, Vol. 111, No. 49, 2007 **12573**

TABLE 1: Structure of MgPc and the MgPc⁻ Anion (Bond Lengths in Å, Angles in Degrees)

bond	ref 4	this work	exp[14]	negative ion
Mg–N$_1$ (Mg–N$_3$)	2.008	1.991	1.990	2.000 (1.991)
N$_1$–C$_1$ (N$_3$–C$_5$)	1.377	1.359	1.386	1.361 (1.367)
N$_2$–C$_1$ (N$_2$–C$_5'$)	1.335	1.317		1.336 (1.307)
C$_1$–C$_2$ (C$_5$–C$_6$)	1.465	1.445	1.411	1.430 (1.451)
C$_2$–C$_2'$ (C$_6$–C$_6'$)	1.415	1.400	1.468	1.411 (1.398)
C$_2$–C$_3$ (C$_6$–C$_7$)	1.395	1.379	1.400	1.385 (1.379)
C$_3$–C$_4$ (C$_7$–C$_8$)	1.397	1.381	1.399	1.377 (1.383)
C$_4$–C$_4'$ (C$_8$–C$_8'$)	1.406	1.392	1.412	1.400 (1.392)
C–H		1.090	1.092	1.121	1.092
θ_{C_1}–N$_1$–C$_1'$ (θ_{C_5}–N$_3$–C$_5'$)	109.7	109.9	109.5	110.1 (110.1)
θ_{N_2}–C$_1$–N$_1$ (θ_{N_2}–C$_5'$–N$_3$)	127.5	127.1	125.9	127.1 (127.8)
θ_{N_1}–C$_1$–C$_2$ (θ_{N_3}–C$_5$–C$_6$)	108.6	108.4	108.9	108.3 (108.0)

3. Neutral MgPc Molecule

The optimized geometry of the neutral MgPc molecule is found to be planar, with structural parameters given in Table 1. They are in good agreement with previous DFT calculation[4] as well as with experimental values.[14] The Kohn–Sham orbitals nearest the Fermi level are displayed in Figure 3. The lowest unoccupied orbital (LUMO) is the 2-fold degenerated e$_g$ orbital, which will later give rise to an open shell problem and a Jahn–Teller effect upon addition of an electron as will be discussed below.

The D_{4h} symmetry of the neutral undistorted molecule implies the decomposition of all $57 \times 3 - 6 = 165$ vibrational modes into irreducible representations

$$\Gamma_{vib} = 14A_{1g} + 13A_{2g} + 14B_{1g} + 14B_{2g} + 13E_g + 6A_{1u} + 8A_{2u} + 7B_{1u} + 7B_{2u} + 28E_u \quad (4)$$

where we note that E$_g$ and E$_u$ are 2-fold degenerate modes. From the electronic structure calculation, the dynamical matrix was obtained by DFT perturbation theory.[24] Molecular vibration eigenvalues and eigenvectors were obtained by diagonalization of the dynamical matrix. The irreducible representation assignment was obtained by constructing projection operators following standard methods.[31] Some of the most intense Raman and Jahn–Teller active modes of MgPc is given in the Table 2. Full table can be found in Supporting Information.[18]

With axes chosen as on Figure 1, the Raman tensors corresponding to the relevant irreducible representation have the form

$$A_{1g}: \begin{pmatrix} a & 0 & 0 \\ 0 & a & 0 \\ 0 & 0 & b \end{pmatrix}$$

$$B_{1g}: \begin{pmatrix} c & 0 & 0 \\ 0 & -c & 0 \\ 0 & 0 & 0 \end{pmatrix}$$

$$B_{2g}: \begin{pmatrix} 0 & d & 0 \\ d & 0 & 0 \\ 0 & 0 & 0 \end{pmatrix}$$

$$E_g: \begin{pmatrix} 0 & 0 & e \\ 0 & 0 & f \\ e & f & 0 \end{pmatrix} \quad (5)$$

The nonzero Raman tensor matrix elements calculated for neutral MgPc are also given in Table 2. We note that because the E$_g$ representation is 2-fold degenerate, it is possible to find a linear combination of the two degenerate modes such that
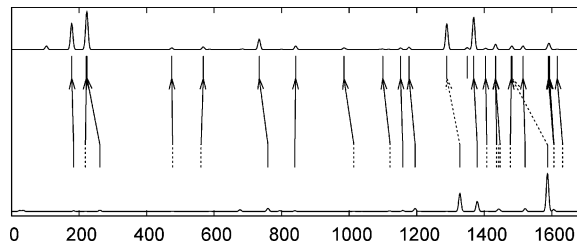
Figure 4. Simulated Raman spectra for neutral (bottom) and charged molecules with fractional occupancy of the e$_g$ levels. Dashed lines mark positions of weak peaks; full lines, strong peaks. Mapping of the modes is indicated by arrows. A dashed arrow indicates the scalar product of the vibrational modes is less than 0.9 (but more than $\sqrt{1/2}$); a full arrow indicates strong similarity.
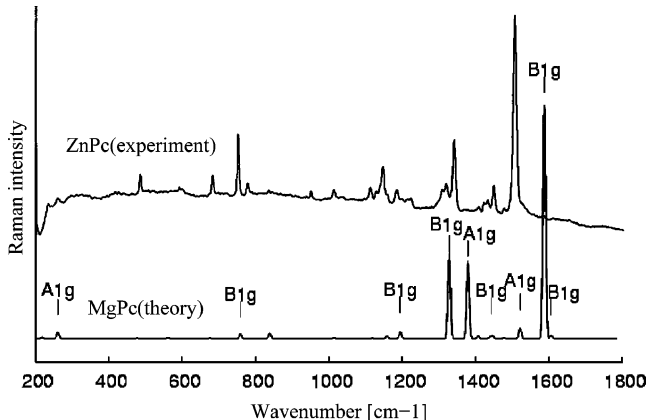
Figure 5. Raman spectra of ZnPc (experimental data from ref 16) and calculated for MgPc.

the Raman tensor for one mode will have only a nonzero T_{xz} element, the other only a T_{yz} element. The value of this element can be chosen as $\sqrt{e^2+f^2}$. We also used the freedom of choice of the sign, corresponding to the choice of the vibration phase.

We observe in our results collected in Table 2 and Figure 4 that the strongest Raman modes predicted in neutral Mg phthalocyanine are high-frequency modes at 1587 and 1328 cm^{-1} (B$_{1g}$ symmetry) and at 1379 cm^{-1} (A$_{1g}$ symmetry).

Conversely, infrared absorption is allowed for A$_{2u}$ and E$_u$ modes. We also give in Table 2 the vibration induced dipole moment amplitudes whose squares are proportional to infrared intensities. Our calculated spectra show a definite similarity with calculated and measured Raman scattering spectra of the other MPcs—mainly ZnPc, which has a similar electronic structure (although possibly without D_{4h} symmetry due to out of plane deformations).[15,16] The nonresonant experimental Raman spectra of ZnPc (with the longest excitation wavelength used, 1064 nm) is compared with our calculated spectra of the MgPc in Figure 5. The level of agreement is only fair, on account of the difference between molecules; nonetheless, there is a good level of correspondence between important groups of modes with dominant intensities.

4. Charged MgPc⁻ Ion

Introducing an electron into the degenerate e$_g$ LUMO leads to a molecular JT distortion with energy lowering. In D_{4h} symmetry the first-order JT active distortions are [e$_g$ × e$_g$] = A$_{1g}$ + B$_{1g}$ + B$_{2g}$ (the square bracket stands for symmetric part of product e$_g$ × e$_g$).

Treating the ion coordinates as classical parameters, and treating spin polarization within the standard LSDA (local spin density approximation), we carried out a full geometry optimi-

TABLE 2: Some of the Most Active Raman or Jahn−Teller Modes of the MgPc Neutral Molecule[a]

frequency	symmetry	Raman intensity	Jahn-Teller parameters
262	A_{1g}	$a = 57.78, b = 5.18$	$k = 0.539, q = 0.0841 \ (0.0774), L = 45.3 \ (41.7)$
477	B_{2g}	$d = 24.06$	$k = 1.271, q = 0.0681, L = 86.5$
589	A_{1g}	$a = 1.28, b = -0.96$	$k = 3.227, q = 0.0287 \ (0.0285), L = 92.6 \ (92.0)$
676	A_{1g}	$a = 20.41, b = -3.83$	$k = 4.321, q = 0.0605 \ (0.0602), L = 261.4 \ (260.1)$
759	B_{1g}	$c = 59.00$	$k = 6.061, q = 0.0393, L = 238.1$
794	B_{1g}	$c = 10.93$	$k = 4.440, q = 0.0247, L = 109.7$
839	A_{1g}	$a = 52.92, b = 8.03$	$k = 5.339, q = 0.0104 \ (0.0082), L = 55.5 \ (43.9)$
934	B_{2g}	$d = 0.38$	$k = 9.163, q = 0.0183, L = 167.7$
1014	A_{1g}	$a = 23.91, b = 3.03$	$k = 1.865, q = 0.0139 \ (0.0161), L = 25.9 \ (30.1)$
1092	B_{2g}	$d = 13.23$	$k = 1.655, q = 0.0414, L = 68.4$
1121	B_{1g}	$c = 12.63$	$k = 1.535, q = 0.0532, L = 81.6$
1158	A_{1g}	$a = 36.42, b = 2.04$	$k = 3.123, q = 0.0286 \ (0.0305), L = 89.2 \ (95.4)$
1195	B_{1g}	$c = 67.84$	$k = 5.271, q = 0.0263, L = 138.4$
1210	B_{2g}	$d = 4.87$	$k = 3.880, q = 0.0587, L = 227.6$
1289	B_{2g}	$d = 14.26$	$k = 3.789, q = 0.0533, L = 202.1$
1328	B_{1g}	$c = 238.92$	$k = 18.812, q = 0.0108, L = 203.4$
1379	A_{1g}	$a = 200.59, b = 2.08$	$k = 23.275, q = 0.0048 \ (0.0060), L = 112.6 \ (140.5)$
1406	B_{1g}	$c = 29.48$	$k = 10.570, q = 0.0170, L = 180.0$
1443	B_{1g}	$c = 33.20$	$k = 7.829, q = 0.0373, L = 292.7$
1447	B_{2g}	$d = 37.92$	$k = 14.366, q = 0.0223, L = 320.7$
1521	A_{1g}	$a = 74.16, b = -1.94$	$k = 23.937, q = 0.0139 \ (0.0123), L = 332.2 \ (295.3)$
1587	B_{1g}	$c = 405.18$	$k = 29.069, q = 0.0443, L = 1287.6$
1606	B_{1g}	$c = 40.20$	$k = 21.857, q = 0.0176, L = 358.3$
1606	A_{1g}	$a = 19.89, b = -1.94$	$k = 20.514, q = 0.0038 \ (0.0040), L = 77.7 \ (81.4)$
1632	B_{2g}	$d = 6.60$	$k = 22.065, q = 0.0067, L = 148.2$

[a] In the first column is the energy of the vibration in cm^{-1}, the next column is the assignment of irreducible representation of the mode (we note that E_g and E_u modes are 2-fold degenerate), and then Raman tensor components for Raman active modes are given in column three. Atomic units are used (Ry for energy, e for charge, a_0 for distance, and amu for mass). Notation of tensor components follows eq 5. The last column contains parameters for the linear Jahn−Teller effect: force constant k in eV/a_0^2, displacement q after addition of one electron in a_0, linear coupling constant L in eV/a_0. For A_{1g} modes it is possible to obtain coupling constants from the position of the minima as well as from the saddle point (in parentheses). The full version of this table is in the Supporting Information.[18]

zation for MgPc$^-$ and found that the distortion is $A_{1g} + B_{1g}$, leading to a reduced D_{2h} symmetry.[32] The JT distorted anion geometry is given in the Table 1. From the total energy difference between the (undistorted) neutral molecule and the distorted negative ion energy, we calculated for MgPc an electron affinity $E_A = 2.06$ eV. This value, similar to that previously calculated for other MPcs,[4] indicates a very substantial electronegativity, albeit not as large as that of C_{60}, where E_A is 2.7 eV. The originally 2-fold degenerate e_g orbital is split into an occupied b_{2g} and an unoccupied b_{3g} (up-spin) Kohn−Sham orbitals. The calculated gap between the two is about 150 meV, most likely an underestimate on account of the gap problem due to self-interaction effects present in DFT.[33] Due to these effects, it is not straightforward to assess the accuracy of the overall energy difference of charged and neutral undistorted molecule. The self-consistent density functional calculation with one electron in 2-fold degenerate orbitals could even fail to converge, especially for very localized orbitals where self-interaction effects are strong. In our case convergence was achieved, but the energy gain is still not to be trusted. We derived a calculated JT distortion energy gain of 50.4 meV (see below) indirectly from the optimal deformation of the molecule (generally more reliable) and the knowledge of its stiffness, under the additional assumption of linearity.[34]

In the limit of strong vibrational coupling where distortion amplitudes can be considered classical variables, the Hamiltonian can be written

$$H = \sum_{i \in \Gamma_{vib}} \frac{1}{2} \left(k_i q_i^2 + \frac{k_i}{\omega_i^2} \dot{q}_i^2 \right) \begin{pmatrix} 1 & 0 \\ 0 & 1 \end{pmatrix} + \sum_{i \in A_{1g}} \begin{pmatrix} 1 & 0 \\ 0 & 1 \end{pmatrix} L_i q_i +$$

$$\sum_{i \in B_{1g}} \begin{pmatrix} 1 & 0 \\ 0 & -1 \end{pmatrix} L_i q_i + \sum_{i \in B_{2g}} \begin{pmatrix} 0 & 1 \\ 1 & 0 \end{pmatrix} L_i q_i \quad (6)$$

The first term is the usual vibrational Hamiltonian including all 165 modes of the molecule. The last three terms represent linear coupling of the symmetry allowed modes, namely, the $14A_{1g}$, $14B_{1g}$, and $14B_{2g}$ modes. The pseudospin matrices represent the electron−phonon interaction with the two-component e_g electronic wave function. By diagonalizing the Hamiltonian (6), we obtain electronic eigenstates for every set of distortion parameters q. In this (Born−Oppenheimer) approximation the corresponding q-dependent total energy represents the potential energy for dynamics in q space. Owing to the double degeneracy of the e_g LUMO, there are two potential energy surfaces (see the Figure 6). They have the form

$$V = \sum_{i \in \Gamma_{vib}} \frac{1}{2} k_i q_i^2 + \sum_{i \in A_{1g}} q_i L_i \pm$$

$$\sqrt{\sum_{i,j \in B_{1g}} L_i L_j q_i q_j + \sum_{i,j \in B_{2g}} L_i L_j q_i q_j} \quad (7)$$

The relevant energy surface will, of course, be the lowest one, corresponding to a minus sign in front of the square root. The double degeneracy is split, and there must be at least one nonzero coordinate q with symmetry B_{1g} or B_{2g} that lowers total energy relative to the conical intersection where $q = 0$. By symmetry, energy (meaning, the anion potential energy surface) has two equivalent minima and two equivalent saddle points. Their coordinates are

$$\vec{q}_m = \left(-\frac{L_{A_{1g}}}{k_{A_{1g}}}, \pm \frac{L_{B_{1g}}}{k_{B_{1g}}}, 0_{B_{2g}} \right)$$

$$\vec{q}_s = \left(-\frac{L_{A_{1g}}}{k_{A_{1g}}}, 0_{B_{1g}}, \pm \frac{L_{B_{2g}}}{k_{B_{2g}}} \right) \quad (8)$$

Electron Doped Metal Phthalocyanines

J. Phys. Chem. A, Vol. 111, No. 49, 2007 **12575**
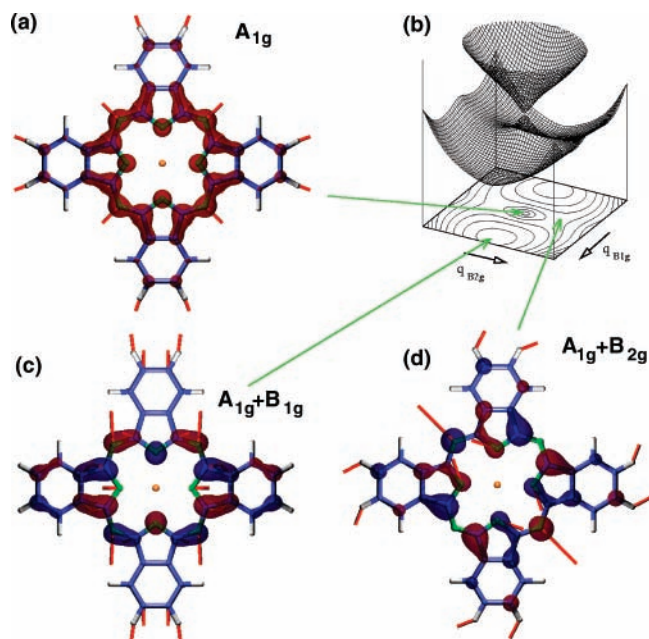
Figure 6. (a) Charge density of two half-occupied e_g orbitals for a symmetric $MgPc^-$ ion. Molecular relaxation caused by the extra electron with respect to the neutral molecule is indicated by red arrows (multiplied by a factor 150). The lower panels represent the negative charge density of the occupied e_g molecular orbitals corresponding to the Jahn−Teller minimum M (c) and saddle point S (d) of the adiabatic potential energy surface (PES). The overall sketch of the PES of this $e_g \times (B_{1g} + B_{2g})$ Jahn−Teller problem is presented on the upper-right panel (b).

where each quantity inside parentheses indicates a set of 14 numbers, one set for each of the three A_{1g}, B_{1g}, and B_{2g} symmetries. We performed the geometry optimization of $MgPc^-$ ion starting from a random deformation of the initial neutral MgPc structure, to which B_{1g} and B_{2g} distortions were added.

We found that the two overall energy minima correspond to a distortion of $B_{1g} + A_{1g}$ symmetry, their q coordinates opposite in sign of the B_{1g} component. The calculated energy gain with respect to the conical intersection (defined as the closest point to 2-fold degeneracy, with coordinates $(-L_{A_{1g}}/k_{A_{1g}}, 0, 0)$), is $E_{JT} = 50.4$ meV. This value of E_{JT} represents our best estimate of the DFT static Jahn−Teller energy of $MgPc^-$, a value quite comparable with that of C_{60}.[35] Conversely, there are two equivalent saddle points corresponding to distortions of $B_{2g} + A_{1g}$ nature. We identified the saddle points by a constrained search where B_{1g} distortions of the molecule were projected out. Again the coordinates of the two saddle points differ just by their sign. Energetically, we found the two B_{2g} distorted saddle points of $MgPc^-$ to lie 23.2 meV below the conical intersection, which means 27.2 meV above the two B_{1g} JT minima. The minimal energy trajectory joining one minimum to the other must negotiate a saddle point, overcoming a barrier of 27.2 meV from either side. The locus of potential energy surface local minima can be qualitatively pictured as a kind of ellipse in the 28-dimensional $B_{1g}-B_{2g}$ plane, as sketched in Figure 6.

Projection of the optimal $MgPc^-$ structure on the original modes of neutral undistorted MgPc yields the JT coupling constants L_i, because these constants uniquely determine the position of the minima given by eq 8 and all the force constants k are known. The coupling constants L thus calculated are given in Table 2. The A_{1g} coupling constants are in fact overdetermined, because they enter to determine both the minimum and

the saddle point. The two determinations agree well as can be seen from the Table 2.

The symmetry of the statically JT distorted $MgPc^-$ molecule is D_{2h}. In the distorted molecule, the set of vibrational modes Γ_{vib} can be decomposed into new irreducible representations

$$\Gamma_{vib} = 28A_g + 27B_{1g} + 13B_{2g} + 13B_{3g} + 13A_u + 15B_{1u} + 28B_{2u} + 28B_{3u} \quad (9)$$

Among these, Raman active modes have A_g, B_{1g}, B_{2g}, and B_{3g} symmetry. Because of the change of molecular symmetry and of the great density of modes, it is difficult to establish the parentage between modes of the neutral and charged molecule. On the other hand, as mentioned earlier, quantum effects should anyway in principle dynamically re-establish an overall D_{4h} symmetry. For this reason we move on to consider alternative approaches, as follows.

5. $MgPc^-$ Symmetrized D_{4h} Ion

The simplest way to crudely simulate the charged molecule retaining its full neutral state symmetry is to ignore the JT effect altogether (because that does not involve a large energy scale), and by forcing the fractional occupancy of both levels to correspond to half an electron each. The allowed deformations in this scheme are then restricted to the A_{1g} symmetry, which preserves the D_{4h} symmetry of the molecule. Independent Raman tensor components again follow eq 5.

The calculated Raman spectral intensities should reasonably apply for nonresonant excitation frequencies well below the HOMO−LUMO gap, which in our LDA calculation of MgPc is $E_{HL} = 1.4$ eV. Figure 4 shows the simulated Raman spectrum obtained with our calculated $MgPc^-$ frequencies and intensities, obtained assuming a Gaussian broadening $\sigma = 5$ cm^{-1} of each peak. We also indicated the frequencies of the negative ion modes, and their parentage between neutral and charged molecule. Parentage was obtained by scalar product between eigenvectors of the neutral and charged molecule, and associating modes whose scalar product is closest to 1. A full line indicates that the scalar product is larger than 0.9, a dashed line indicates scalar product between 0.9 and $\sqrt{1/2}$. The full calculated vibrational spectra and Raman and infrared absorption intensities are tabulated for reference as Supporting Information.[18] Although each mode has its individual behavior, we note a general downward vibrational frequency shift upon doping, which will be briefly discussed below.

6. Discussion and Conclusions

We have presented calculations of structure, energetics, vibrational, and Raman spectra of the neutral MgPc molecule, and of the negatively charged $MgPc^-$ molecular ion. We found no Raman data for MgPc, and our calculations therefore stand as a reference for future measurements. The theoretical Raman spectrum of neutral MgPc compares reasonably well with spectra of ZnPc measured and calculated by Tackley et al.,[15,16] which is reasonable in view of the similarity of electronic structures of MgPc and ZnPc.

In the negative ion $MgPc^-$ we considered the JT effect and found that the JT energy and the barriers between equivalent minima are relatively small. That suggests the existence of important dynamical JT phenomena, to be pursued elsewhere. We found the static JT energy gain to be 50.4 meV, much smaller with respect to an earlier estimated value of 322 meV (2600 cm^{-1}).[12] The disagreement is not surprising, in view of the early work's excessive structural constraints on aza or

pyrrole nitrogen distortions, related also to an apparently incorrect identification of the symmetry allowed JT modes (quoted as E_g instead of B_{1g} and B_{2g}). Moreover, where DFT might tend to underestimate somewhat the distortion energies, the Hartree−Fock method tends to overestimate them due to its lack of correlations effects. The measured photoabsorption spectra of the MgPc$^-$ anion[36] analyzed in ref 12 were interpreted in terms of a hypothetical JT splitting of the e_g orbital of about 37 meV (300 cm^{-1}). Cory et al. in fact calculated that splitting to be 174 meV (1400 cm^{-1}) by INDO/1 or 372 meV (3000 cm^{-1}) by Hartree−Fock. Our DFT calculated energy splitting between occupied spin-up b_{3g} and unoccupied spin-up b_{2g} orbital is 126 meV. Because LDA usually tends to underestimate real gaps, we suspect a possible misinterpretation of the 37 meV feature, which could rather correspond to some vibronic transition, as could be checked after solving the full dynamical Jahn−Teller problem.

Our overall result is that although individual modes behave differently upon doping, charging generally downshifts the vibrational frequencies of MgPc. From Figure 4 we can see that most Raman active modes above 700 cm^{-1} downshift by about 10 cm^{-1}. This shift only represents a crude average value, for example, the B_{1g} mode at 759 cm^{-1} shifts to 733 cm^{-1} upon doping by one electron. This mode seems to have stable intensity and is not too close to other intense Raman peaks, so it could serve as a reasonable reference. Other peaks with noticeable intensity and relatively stable upon charging are the B_{1g} mode at 1195 cm^{-1} with a shift of −18 cm^{-1} and the A_{1g} mode at 1379 cm^{-1} with a predicted shift of −10 cm^{-1}. The latter contains the isotropic as well as anisotropic part of Raman scattering; therefore it can be distinguished from others by changing the geometry of the experiment (see formula 1 and comments below). We suggest these three modes might constitute good indicators for charge transfer, because they have observable intensity and preserve their own character upon charging.

Recent Raman data on CuPc and KCuPc show peak shifts from 1452 to 1443 cm^{-1} and from 748 to 737 cm^{-1}[13] (read from Figure 4). These shifts were measured on samples with uncertain charge transfer, probably not very different from one electron per CuPc molecule.

Although CuPc is of course far from identical to MgPc, it is found theoretically that, as in MgPc, the extra electron goes entirely in the e_g LUMO.[4] It seems thus plausible that these three CuPc Raman modes might be compared to our calculated ones for MgPc and that the observed doped-related frequency shift could in fact indicate a qualitative measure of the doping level, on the order of 1 electron/molecule. It will be interesting to consider future experiments that could check our predictions with variable electron fillings.

Supporting Information Available: Full vibration spectra of neutral MgPc and charged MgPc$^-$ molecules, together with calculated Infrared and Raman scattering intensities. This information is available free of charge via the Internet at http://pubs.acs.org.

References and Notes

(1) Ishiguro, T.; Yamaji, K.; Saito, G. *Organic Superconductors*, 2nd ed.; Springer: Berlin, 1998.

(2) Craciun, M. F.; Rogge, S.; Wismeijer, D. A.; den Boer, M. J. L.; Klapwijk, T. M.; Morpurgo, A. F. In *Proceedings of the 12th International Conference on Scanning and Tunneling Microscopy/Spectroscopy and Related Techniques*; Koenraad, P. M., Kemerink, M., Eds.; AIP Conference Proceedings; AIP: Woodbury, NY, 2003; No. 696, p 489.

(3) Craciun, M. F.; Rogge, S.; den Boer, M. J. L.; Margadonna, S.; Prassides, K.; Iwasa, Y.; Morpurgo, A. F. *Adv. Mater.* **2006**, *18*, 320.

(4) Liao, M. S.; Scheiner, S. *J. Chem. Phys.* **2001**, *114*, 9780.

(5) In addition, in the transition metal MPcs examined by Craciun *et al.*, the chemical potential must be in equilibrium with a partly filled metal d-level. Strongly localized, this orbital should possess a much larger on-site Coulomb repulsion and must constitute a nontrivial magnetic complication, which is absent in MgPc. The interplay of metallic conduction in the LUMO with the localized d-level will no doubt generate future interest in transition metal MPcs as mixed valent systems with either double exchange or Kondo intramolecular couplings.

(6) Tosatti, E.; Fabrizio, M.; Tóbik, J.; Santoro, G. E. *Phys. Rev. Lett.* **2004**, *93*, 117002.

(7) MnPc, FePc, CoPc, and CuPc are open shell molecules,[4] so that the pristine parent insulators themselves constitute single-band Mott−Hubbard insulators.

(8) Murphy, D. W.; Rosseinsky, M. J.; Fleming, R. M.; Tycko, R.; Ramirez, A. P.; Haddon, R. C.; Siegrist, T.; Dabbagh, G.; Tully, J. C.; Walstedt, R. E. *J. Phys. Chem. Solids* **1992**, *53*, 1321. Ramirez, A. P. *Superconductivity Rev.* **1994**, *1*, 1. Margadonna, S., Ed. *Chemistry and Physics of Fullerenes*; Springer: Berlin, 2006. Gunnarsson, O. *Alkali Doped Fullerides*; World Scientific: Singapore, 2005.

(9) Bozio, R.; Zanon, I.; Girlando, A.; Pecile, C. *J. Chem. Phys.* **1979**, *71*, 2282.

(10) Modesti, S.; Cerasari, S.; Rudolf, P. *Phys. Rev. Lett.* **1993**, *71*, 2469.

(11) Iwasa, Y.; Shimoda, H.; Takenobu, T.; Honjo, S.; Mitani, T.; Tou, H.; Maniwa, Y.; Brown, C. M.; Prassides, K. *Fullerene Sci. Technol.* **1999**, *7*, 587.

(12) Cory, M. G.; Hirose, H.; Zerner, M. C. *Inorg. Chem.* **1995**, *34*, 2969.

(13) Mihil, A.; Buel, W.; Fink, M. *J. Chem. Phys.* **1993**, *99*, 6416.

(14) Ruan, C.-Y.; Mastryukov, V.; Fink, M. *J. Chem. Phys* **1999**, *111*, 3035.

(15) Tackley, D. R.; Dent, G.; Smith, W. E. *Phys. Chem. Chem. Phys.* **2000**, *2*, 3949.

(16) Tackley, D. R.; Dent, G.; Smith, W. E. *Phys. Chem. Chem. Phys.* **2001**, *3*, 1419.

(17) Jancziak, J.; Kubiak, R. *Polyhedron* **2001**, *20*, 2901.

(18) Adittional data not published in this paper can be found in the Supporting Information.

(19) See, for example: Englman, R. *The Jahn-Teller effect in molecules and crystals*; Wiley: New York, 1972.

(20) Baroni, S.; Dal Corso, A.; de Gironcoli, S.; Giannozzi, P. http://www.pwscf.org.

(21) Rappe, A. M.; Rabe, K. M.; Kaxiras, E.; Joannopoulos, J. D. *Phys. Rev. B* **1990**, *41*, 1227.

(22) Mermin, N. D. *Phys. Rev.* 1**965**, *137*, A1441.

(23) Marzari, N.; Vanderbilt, D.; Payne, M. C. *Phys. Rev. Lett.* **1997**, *79*, 1337.

(24) Baroni, S.; de Gironcoli, S.; Dal Corso, A.; Giannozzi, P. *Rev. Mod. Phys.* **2001**, *73*, 515.

(25) See, for example: Long, D. A. *Raman Spectroscopy*; McGraw-Hill: New York, 1977.

(26) Tóbik, J.; Dal Corso, A. *J. Chem. Phys.* **2004**, *120*, 9934.

(27) Deinzer, G.; Strauch, D. *Phys. Rev. B* **2002**, *66*, 100301.

(28) Lazzeri, M.; Mauri, F. *Phys. Rev. Lett.* **2003**, *90*, 036401.

(29) Porezag, D.; Pederson, M. R. *Phys. Rev. B* **1996**, *54*, 7830.

(30) Wilson, E. B.; Decius, J. C.; Cross, P. C. *Molecular Vibrations*; McGraw-Hill: New York, 1955.

(31) See, for example: Inui, T.; Tanabe, Y.; Onodera, Y. *Group Theory and Its Applications in Physics*, 2nd ed.; Springer-Verlag: Berlin, 1996.

(32) Tóbik, J.; Tosatti, E. *J. Mol. Struct.* **2007**, *838*, 112.

(33) Jones, R. O.; Gunnarsson, O. *Rev. Mod. Phys.* **1989**, *61*, 689.

(34) We note that besides the distortion induced b_{3g}↑−b_{2g}↑ splitting of 126 meV, there is also an exchange splitting of 149 meV for the b_{3g} level and of 49 meV for the b_{2g} level. There are also spin splittings of smaller magnitude of all other occupied states.

(35) See, for example: Manini, N.; Dal Corso, A.; Fabrizio, M.; Tosatti, E. *Philos. Mag. B* **2001**, *81*, 793. Manini, N.; Tosatti, E. In *Chemistry and Physics of Fullerenes*; Margadonna, S., Ed.; Springer: Berlin, 2006.

(36) Mack, J.; Kirkby, S.; Ough, E. A.; Stillman, M. *J. Inorg. Chem.* **1992**, *31*, 1717.